PCCP

Molecules mimicking atoms: Monomers and dimers of alkali metal solvated electron precursors

Journal:	*Physical Chemistry Chemical Physics*
Manuscript ID	CP-ART-08-2018-005497
Article Type:	Paper
Date Submitted by the Author:	29-Aug-2018

Complete List of Authors:	Ariyarathna, Isuru; Auburn University, Chemistry and Biochemistry Pawlowski, Filip; Auburn University, Chemistry and Biochemistry Orti, J.Vincent; Auburn University, Chemistry and Biochemistry Miliordos, Evangelos; Auburn University, Chemistry and Biochemistry

Molecules mimicking atoms: Monomers and dimers of alkali metal solvated electron precursors

Isuru R. Ariyarathna, Filip Pawłowski, Joseph Vincent Ortiz, and Evangelos Miliordos*

Department of Chemistry and Biochemistry, Auburn University, Auburn, AL 36849

Abstract

Tetra-amino lithium and sodium complexes $M(NH_3)_4^{0,-}$ (M=Li, Na) have one or two electrons that occupy diffuse orbitals distributed chiefly outside the $M(NH_3)_4^+$ core. The lowest-energy 1s, 1p, and 1d orbitals follow Aufbau principles found earlier for beryllium tetra-ammonia complexes. Two ground state $M(NH_3)_4$ complexes can bind covalently by coupling their $1s^1$ electrons into a σ-type molecular orbital. The lowest excited states of the $[M(NH_3)_4]_2$ species are obtained by promoting one or two electrons from this σ to other bonding or anti-bonding σ and π-type molecular orbitals. The electronic structure of solvated electron precursors provides insights into chemical bonding between super-atomic species that are present in concentrated alkali-metal-ammonia solutions.

* To whom correspondence should be addressed. E-mail: emiliord@auburn.edu

TOC GRAPHIC

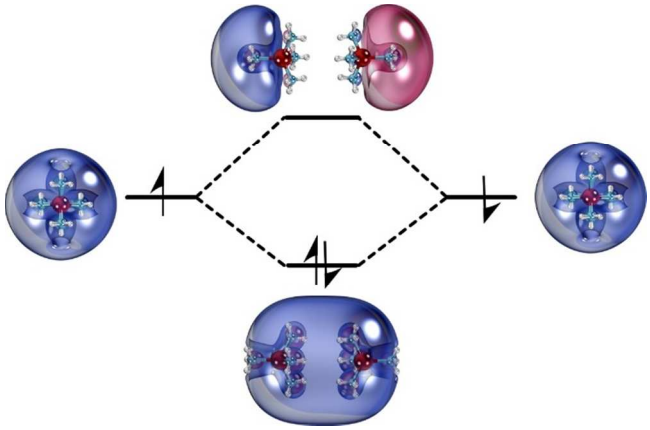

I. Introduction

The addition of alkali metals into liquid ammonia is known to produce solvated electrons (e^-_{solv}) and positively charged metal-ammonia coordination complexes (M^+_{solv}).[1] Increase of the metal concentration causes the formation of $M^+_{solv}e^-_{solv}$ ion pairs, also called solvated electron precursors (SEP).[2] A SEP is a complex that displaces one or more electrons from its coordinated metal atom to the periphery of its ligands. At higher concentrations, M^+_{solv} binds an electron pair making M^-_{solv} or SEPs form dimers ($M^+_{solv}e^-_{solv}-M^+_{solv}e^-_{solv}$). Finally, very dense solutions conduct like a metal rather than an electrolyte, signaling the formation of crystal-like, liquid-metal structures.[1,3-6] Recently, similar electric and structural properties were observed for lithium-ammonia-methyl ammonia mixtures.[7]

In an effort to better comprehend the electronic structure of the species present in intermediate concentrations, we perform high-level quantum chemical calculations on isolated SEPs, their anions, and their dimers. We elucidate the electronic spectrum of all of these species and provide accurate excitation energies and structural information. The presently reported data are expected to facilitate additional ways, such as spectroscopic methodologies, to identify these species in the gas or condensed phases. Presently, we examine the two smallest alkali-metal atoms in an attempt to identify possible differences between them and clarify the role of the central metal. Does the metal change the electronic spectrum of its SEP? Do the binding energies of the two Li-SEP and Na-SEP monomers differ? Would different binding energies for the two SEP dimers mean that the formation of one of them is less likely in solution?

Recently, we worked on beryllium ammonia complexes such as $Be(NH_3)_3$,[8] and $Be(NH_3)_4$.[2] We found that $Be(NH_3)_3$ demonstrates different bonding patterns than other tri-coordinated beryllium complexes. Specifically, $Be(CX)_3$ and $Be(PH_3)_3$ induce the excitation of the ground state Be($^1S;2s^2$) to its sixth excited state Be($^1D;2p^2$), while $Be(NH_3)_3$ prefers to "solvate" the $2s^2$ electron pair in its periphery. This solvation process is more profound for the beryllium SEP and its ions, $Be(NH_3)_4^{0,\pm}$, for which we calculated the ground and a series of excited electronic states.[2] We discovered that for all three species there is a $Be(NH_3)_4^{2+}$ core which hosts up to three electrons on its periphery. These outer electrons occupy diffuse atomic-

like orbitals which do not follow the hydrogenic Aufbau principle. The lowest energy orbitals are 1s, 1p, 1d, 2s, 1f, and 2p (see Figure 1). We proved that this sequence of orbitals is caused by the electrostatic potential experienced by the outer electrons. Here we examine the $Li(NH_3)_4$ and $Na(NH_3)_4$ SEPs, which have an $M(NH_3)_4^+$ (M = Li, Na) core and one outer electron, as well as their anions and dimers.

Both experimental[9-12] and theoretical[13-19] work has been devoted to lithium and sodium ammonia clusters in the literature. Previous studies focus on the micro-solvation process and how valence electrons migrate from the metal to remote solvent molecules. We are aware of only three theoretical studies that report two low-lying excited states of $Li(NH_3)_4$ and $Na(NH_3)_4$.[1,16,17] Here we report a larger number of excited states and we investigate the bonding between two SEPs. We see that two SEPs bind similarly to diatomic molecules and form molecular orbitals of σ- and π-type symmetry.

In Section II we describe our computational approach, in Sections III and IV we discuss our results on the SEP monomers and dimers, respectively, and in Section V we summarize our findings.

II. Computation details

A variety of *ab initio* methods have been applied to the ground and excited states of $M(NH_3)_4$. Ground state structures were optimized with coupled-cluster singles, doubles and perturbative triples [CCSD(T)][20] total energies. With density functional theory (B3LYP),[21,22] these structures were re-optimized and all real harmonic vibrational frequencies were calculated [see Electronic Supplementary Information (ESI)].

Complete-active-space, second-order perturbation theory (CASPT2) produced accurate vertical excitation energies. All valence electrons are correlated to describe dynamic correlation. The reference wavefunction was built at the complete active space self-consistent field (CASSCF) level. The active space consists only of outer orbitals and electrons, and the exact kind of orbitals included for each system is discussed in Sections III and IV. Electron affinities

of cations were calculated with the renormalized partial third-order quasiparticle (P3+) electron propagator method[23] (see ESI), and vertical excitation energies of doublet molecules were inferred from differences of these electron binding energies.

Our earlier work on beryllium[2] revealed that double diffuse functions on the terminal hydrogen atoms are important and that the contribution of diffuse functions on the metal or nitrogen is minimal. Very similar conclusions were drawn recently by Palmer et al. who studied Rydberg states of difluoromethane. The optimum position for the diffuse functions was found to be the terminal hydrogen atoms.[24] Excitation energies for low-lying states of $Be(NH_3)_4$ were practically converged with the following correlation-consistent basis set[25,26] combination: cc-pVTZ for the metal and nitrogen, and d-aug-cc-pVTZ for all hydrogen centers. We employ this combination for the calculations of the vertical excitation energies, but aug-cc-pVTZ on all atoms for the geometry optimization of the ground states. The diffuse functions were found to be necessary for accurate excitation energies and the prediction of stable anionic species (see ESI).

All calculations were done under C_{2v} symmetry. The MOLPRO[27] and Gaussian[28] electronic structure codes were invoked. The computational details for the dimers will be given below.

III. The lithium and sodium SEP monomers

CCSD(T) optimizations produce tetrahedral minima for all molecular species $M(NH_3)_4^{0,\pm}$, the ground states of which have zero, one or two outer electrons in the pseudo-spherical 1s orbital (see Figure 1). The optimal geometries are given in Table 1. Observe that the metal-nitrogen distance contracts appreciably when at least one outer electron is present. For both metals, the distance in $M(NH_3)_4^{0,-}$ is about 0.03 Å shorter than in the naked $M(NH_3)_4^{+}$ complexes, but the N-H bonds elongate by only 0.003 Å. A strong attraction between the central metal and the first outer electron pulls the ammonia ligands closer to the metal. Addition of another electron in the anion produces more diffuse outer orbitals and therefore the M-N distances are almost unchanged.

The ionization energies of the Li and Na tetra-ammonia complexes (2.92 and 2.79 eV) are about half of those of the corresponding metal atoms (5.39 and 5.14 eV)[29] and approximately twice as large as those of solvated atoms (1.47 and 1.66 eV).[10,12] edw The electron affinities of plain Li and Na are 0.62 and 0.55 eV,[29] whereas those of the ammonia complexes are smaller (0.45 eV for both). In the case of Be, we noticed the opposite effect. The electron affinity for the $Be(NH_3)_4$ complex is 0.26 eV, but Be^- is not stable.[2]

Lithium makes stronger ammonia complexes than sodium. The binding energies of all four ammonia ligands to the metal are 56.8 and 31.8 kcal/mol for Li and Na, which become 50.6 and 26.7 kcal/mol after zero-point-energy (ZPE) corrections. We plotted the potential energy curve (PEC) with respect to the metal-nitrogen distance pertaining to the simultaneous approach of the four ligands. The PECs shown in Figure 2 decrease monotonically from infinity to equilibrium without the barrier that occurred in the Be case, where there are two valence electrons instead of one.[2] We next studied the abstraction of one ammonia molecule from the complex leading to the lower energy $M(NH_3)_3$+NH_3 asymptote. These PECs are also monotonic for alkali-metals, but their beryllium counterparts also had a small energy barrier. The ZPE-corrected binding energies are 9.4 and 7.4 kcal/mol for Li and Na.

Table 2 lists the vertical excitation energies for ten electronic states for both systems at the CASSCF, CASPT2 and P3+ levels. In all cases, CASSCF underestimates them by 0.2-0.3 eV. Our CASSCF active space consists of 1 electron in 24 orbitals ($9a_1$, $6a_2$, $6b_1$, $3b_2$ under C_{2v}). All 24 orbitals are outer orbitals, but all valence electrons (including those of the $M(NH_3)_4^+$ core) are correlated at the CASPT2 level. The ground state (1^2A_1) for both complexes has a $1s^1$ configuration. The first excited state corresponds to a sextuply degenerate state 1^2T_2 ($1p^1$) that is 0.72 (Li) or 0.65 (Na) eV higher. The $1d^1$ configuration splits to the 2^2T_2 and 1^2E states, which are practically degenerate. All $1d^1$ components lie within 0.03 eV of each other for both species. In the next state (2^2A_1), the electron occupies the 2s orbital, while the 3^2T_2 state follows with a $2p^1$ configuration. In the outer orbitals of the remaining four states (1^2T_1, 4^2T_2, 2^2E, and 5^2T_2), functions of different angular momenta mix considerably.

CASPT2 and P3+ excitation energies are in excellent agreement for lower lying states and produce the same Aufbau principle for diffuse electrons. Hashimoto and Daigoku's MP2 calculations on $Li(NH_3)_4$ located two doublet excited states, at 0.62 and 1.54 eV,[16,17] which match well with our 1^2T_2 and 2^2A_1 predictions. Numerical discrepancies between CASPT2 and

P3+ excitation energies may be larger for certain higher states and could be consequences of incomplete basis sets in those cases.

The transition dipole moments (μ_T) between the ground state $^2A_1$ ($1s^1$) and all excited states, except the $^2T_2$ ones, are zero by symmetry. The μ_T^2 values for 1^2T_2 ($1p^1$) and 2^2T_2 ($1d^1$) are 177/189 and 0.01/0.05 D^2 (Li/Na), respectively. These data approach atomic selection rules where the 1s→1p transition is allowed, unlike 1s→1d. Similarly, among the states of Table 2 only 1s→2p (3^2T_2) has a small non-zero μ_T^2 value (0.2/0.5 D^2).

The largest amplitudes of the orbitals of Figure 1 occur outside the covalent radii of the atoms, especially on the periphery of the complex, and differ significantly from those of valence or Rydberg orbitals of the metal atoms. Regions outside the covalent radii include interstices between ammonia ligands. Orthogonality to lower, occupied orbitals produces minor amplitudes within the covalent radii. Similar conclusions on the 1s orbital have followed from analysis in terms of metal and ligand fragment orbitals[1] or spatial distributions of natural orbitals.[30] Although the two parent metals have different energy level patterns ($2s^1$, $2p^1$, $3s^1$, $3p^1$, $3d^1$ for Li versus $3s^1$, $3p^1$, $3d^1$, $4s^1$, $4p^1$, $4d^1$, $4f^1$ for Na), they adopt the same shell model after coordination. This complex pattern of interference arises from an electrostatic potential that is not hydrogenic and which generates the relatively simple Aufbau rules summarized in Figure 1 and Table 2.

IV. The lithium and sodium SEP dimers

The $M(NH_3)_4$ systems have an unpaired electron orbiting around the $M(NH_3)_4^+$ core as in the hydrogen atom. Pushing two such complexes together, we expect to see the formation of a covalent bond. Indeed, the binding energies of $[M(NH_3)_4]_2$ were found to be practically the same for the two metals with B3LYP: 9.1 (M = Li) and 9.5 (M = Na) kcal/mol. For M = Li, we also obtained the CASPT2 optimal geometry which is shown in Figure 3. The CASPT2 binding energy for lithium is 14.7 kcal/mol, 5.6 kcal/mol larger than B3LYP. The optimal structures for both dimers are given in the ESI. The basis set used for the dimers is cc-pVTZ for the metal and nitrogen, and aug-cc-pVTZ for hydrogen.

Three ammonia ligands of each monomer stay in the middle in a staggered conformation and hydrogen atoms from different monomers approach each other in a D_{3d} structure. The reason

for these contacts is the electronic density in the middle of the two monomers resulting from the formation of a σ-covalent bond. Zurek et al. considered more relative orientations of the two monomers, which were found to be nearly degenerate.[1] Our structure is not reported by these authors and it is lower in energy than all of theirs at the B3LYP level. Our geometry optimizations using their geometries as initial guesses converged to our structure, which has only real frequencies (see ESI). To rule out any artifacts due to the basis set incompleteness, we employed also quadruple quality-ζ basis sets, which showed the exact same trends. Tight convergence criteria needed to be applied to obtain optimal structures without imaginary frequencies.

In all of the structures, the density of the diffuse electron pair is concentrated in the middle of the two $M(NH_3)_4^+$ cores (see Figure 23 of ref. 1 and present Figure 4). Among all of the structures, the D_{3d} one contains the larger number of O-H bonds interacting with the diffuse electron pair and this electrostatic attraction seems to be the reason for its additional stability.

Selected molecular orbitals of the structure of Figure 3 are depicted in Figure 4. These functions have shapes that are similar to those of typical diatomic molecules: $1a_{1g} \sim 1s_A + 1s_B$, $1a_{2u} \sim 1s_A - 1s_B$, $2a_{1g} \sim 1p_{z,A} - 1p_{z,B}$, $2a_{2u} \sim 1p_{z,A} + 1p_{z,B}$, $1e_u \sim (1p_{x,A} + 1p_{x,B}$ or $1p_{y,A} + 1p_{y,B})$, and $1e_g \sim (1p_{x,A} - 1p_{x,B}$ or $1p_{y,A} - 1p_{y,B})$. Identical observations can be made for sodium. The a_{1g}, a_{2u}, e_g, and e_u orbitals imitate the σ_g, σ_u, π_g, π_u orbitals of homonuclear diatomics.

PECs as a function of the distance between the two monomers for Li are plotted in Figure 5. At every Li-Li distance, we optimize all other geometrical parameters with B3LYP for the ground state but impose the D_{3d} symmetry of the global minimum. We use these geometries to obtain the PECs of the excited states at CASPT2. The large computational cost constrained us to use only the 1s and 1p super-atomic orbitals of each monomer (see Figure 1) in the CASSCF active space. All valence electrons are correlated at CASPT2.

The lowest two asymptotic channels are $1^2A_1(1s^1) + 1^2A_1(1s^1)$ and $1^2A_1(1s^1) + 1^2T_2(1p^1)$. The former generates one singlet (1^1A_{1g}) and one triplet (1^3A_{2u}). These states resemble the $^1\Sigma_g^+$ and $^3\Sigma_u^-$ states of H_2 arising from the ground state fragments $H(^2S) + H(^2S)$ and their equilibrium configurations are $1a_{1g}^2$ and $1a_{1g}^1 1a_{2u}^1$. The next channel is the analogue of $H(^2S)+H(^2P)$, which gives singlets and triplets of $\Sigma_{g,u}$ and $\Pi_{g,u}$ symmetry. In our case we obtained the corresponding D_{3d} representations: $^{1,3}A_{1g}$, $^{1,3}A_{2u}$, $^{1,3}E_u$, and $^{1,3}E_g$. The $^1A_{2u}$ (1^1A_{2u}) state is the open-singlet counterpart of 1^3A_{2u}. The equilibrium electronic configurations of the remaining states are given

in Table 3. The global minima of all of our PECs occur at 6-8 Å, but have shoulders (or shallow minima in some cases) in the typically repulsive region around 4 Å. These features may arise from the complex electrostatics of the system or from avoided crossings with higher channels (see below).

The next dissociation channel should be $1^2A_1(1s^1) + 2^2T_2(1d^1)$ at 1.40 eV followed by $1^2T_2(1p^1) + 1^2T_2(1p^1)$ at 1.44 eV (see Table 2). Because of our 1s1p active space, we were not able to capture the $2^2T_2(1d^1)$ channel. We managed however to locate one of the PECs of $^1A_{1g}$ symmetry stemming from the ionic fragments $Li(NH_3)_4^+$ ($^1A_1$) + $Li(NH_3)_4^-$ ($^1A_1$); see Figure 5. There is one more $^1A_{1g}$ state in between coming from $1^2T_2(1p^1) + 1^2T_2(1p^1)$ which undergoes an avoided crossing with the ionic one. We cannot rule out the possibility that the shoulders of our PECs at 4 Å are related to different ionic channels.

Identical conclusions can be deduced from the more demanding calculations performed on $[Na(NH_3)_4]_2$. Due to technical issues we were able to construct a smaller number of PECs shown in Figure 6. The PECs of the states in common are of similar shape and have almost identical potential well depths.

Vertical excitation energies for the two dimers are listed in Table 3. These energies are slightly different from those of Figure 5 and 6 because of the different number of states averaged at the CASSCF level. In Figures 5 and 6, we included more states to ensure the smoothness of the PECs, but in Table 3 we have state-averaged only those listed and these values are more accurate. For $[Li(NH_3)_4]_2$ we used both the CASPT2 and DFT/B3LYP optimal structures of the ground state. The values differ by less than 0.13 eV. The excitation energies for sodium are lower than those of lithium, as happens for the monomers. The energy difference is consistently lower by 0.2-0.3 eV for the states studied here.

V. Conclusions

Ground and excited electronic states of the lithium and sodium tetra-ammonia complexes were investigated by means of high-level quantum chemical calculations. We found that a neutral complex has an $M(NH_3)_4^+$ core and one electron orbiting in its periphery that occupies s,

p, d, or higher *l*-type orbitals. The orbital sequence is the same for both metals and identical to that which we found for $Be(NH_3)_4^{0,\pm}$ complexes and which resembles that of the jellium or nuclear shell model.[2] We demonstrated that the central metal acts more like a point charge and that it does not affect the shell model of the corresponding SEP. For both metals, the $M(NH_3)_4^+$ core can bind a second electron by 0.45 eV to form an anion.

We finally show that two $M(NH_3)_4$ complexes can form a single covalent σ-bond by coupling their unpaired electrons into a closed shell singlet. The binding energy for the two metals is practically identical implying that SEP dimers will be formed in both cases at similar concentrations. Excited states of the dimer involve electronic excitations to other σ- or π-type orbitals similar to those of typical diatomic molecules. The electronic spectrum of these dimers is also largely independent of the central metal. Our results reveal the ability of SEPs to form covalently bound aggregates which can lead to novel liquid-metal materials or chemical compounds made of SEPs.

Acknowledgements

IRA and EM are indebted to Auburn University for financial support. This work was completed in part with resources provided by the Auburn University Hopper Cluster. JVO acknowledges the support of the National Science Foundation through grant CHE-1565760 to Auburn University.

References

(1) E. Zurek, P. P. Edwards and R. Hoffmann, *Angew. Chem. Int. Ed.* 2009, **48**, 8198-8232.

(2) I. R. Ariyarathna, S. N. Khan, F. Pawłowski, J. V. Ortiz and E. Miliordos, *J. Phys. Chem. Lett.* 2018, **9**, 84-88.

(3) U. Pinsook and S. Hannongbua, *J. Chem. Phys.* 2006, **124**, 074702.

(4) G. N. Chuev and P. Quémerais, *J. Chem. Phys.* 2008, **128**, 144503.

(5) E. Zurek, X. -D. Wen and R. Hoffman, *J. Am. Chem. Soc.* 2011, **133**, 3535-3547.

(6) A. G. Seel, E. Zurek, A. J. Ramirez-Cuesta, K. R. Ryan, M. T. J. Lodge, and P. P. Edwards, *Chem. Comm.* 2014, **50**, 10778-10781.

(7) A. G. Seel, H. Swan, D. T. Bowron, J. C. Wasse, T. Weller, P. P. Edwards, C. A. Howard and N Skipper, *Angew. Chem. Int. Ed.* 2017, **56**, 1561-1565.

(8) I. R. Ariyarathna and E. Miliordos, *Int. J. Quantum Chem.* 2018, XX, XXXX, DOI: 10.1002/qua.25673

(9) I. V. Hertel, C. Hüglin and C. Nitsch, *Phys. Rev. Lett.* 1991, **67**, 1767-1770.

(10) R. Takasu, K. Hashimoto and K. Fuke, *Chem. Phys. Lett.* 1996, **258**, 94-100.

(11) R. Takasu, F. Misaizu, K. Hashimoto and K. Fuke, *J. Phys. Chem. A* 1997, **101**, 3078-3087.

(12) C. Steinbach and U. Buck, *J. Chem. Phys.* 2005, *122*, 134301.

(13) K. Hashimoto and K. Morokuma, *J. Am. Chem. Soc.* 1995, **117**, 4151-4159.

(14) Y. Ferro, A. Allouche and V. Kempter, *J. Chem. Phys.* 2004, **120***,* 8683-8691.

(15) G. Gao and Z. –F. Liu, *J. Chem. Phys.* 2007, **126**, 084501.

(16) K. Hashimoto and K. Daigoku, *Phys. Chem. Chem. Phys.* 2009, **11**, 9391-9400.

(17) K. Hashimoto and K. Daigoku, *Chem. Phys. Lett.* 2009, **469**, 62-67.

(18) H. Zhang and Z. –F. Liu, *J. Chem. Phys.* 2012, **136**, 124314.

(19) N. V. Kryzhevoi, F. Tarantelli and L. S. Cederbaum, *Chem. Phys. Lett.* 2015, **626**, 85-89.

(20) K. Raghavachari, G. W. Trucks, J. A. Pople and M. Head-Gordon *Chem. Phys. Lett.* 1989, **157**, 479-483.

(21) C. Lee, W. Yang and R. G. Parr, *Phys. Rev. B* 1988, **37**, 785-789.

(22) A. D. Becke *J. Chem. Phys.* 1993, *98*, 5648-5652.

(23) H. H. Corzo and J. V. Ortiz, *Adv. Quantum Chem.* 2017, **74**, 267-98.

(24) M. H. Palmer, S. V. Hoffmann, N. C. Jones, M. Coreno, M. de Simone, C. Grazioli, *J. Chem. Phys.* 2018, **148**, 214304.

(25) T. H. Dunning, *J. Chem. Phys.* 1989, **90**, 1007-1023.

(26) R. A. Kendall, T. H. Dunning and R. J. Harrison, *J. Chem. Phys.* 1992*,* **96**, 6796-6806.

(27) H.-J. Werner, P. J. Knowles, G. Knizia, F. R. Manby, M. Schütz, et al. *MOLPRO*, version 2015.1, a package of ab initio programs; see http://www.molpro.net [Accessed: 5/24/2018].

(28) *Gaussian 16, Revision A.03* M. J. Frisch, G. W. Trucks, H. B. Schlegel, G. E. Scuseria, M. A. Robb, et al. *Gaussian Inc., Wallingford CT, 2016.*

(29) W. M. Haynes, (Editor-in-chief) *CRC Handbook of Chemistry and Physics*, 92nd ed. CRC Press: USA; 2012.

(30) T. Sommerfeld and K. M. Dreux, *J. Chem. Phys.* 2012, **137**, 244302.

Table 1. CCSD(T) optimized M-N and N-H bond distances (Å), M-N-H angles (degrees), and relative energies ΔE (eV) for M = Li and Na.

Species	M-N	N-H	M-N-H	ΔE
$Li(NH_3)_4^+$	2.109	1.017	113.6	2.92
$Li(NH_3)_4$	2.078	1.020	112.8	0.0
$Li(NH_3)_4^-$	2.079	1.020	112.8	−0.45
$Na(NH_3)_4^+$	2.504	1.017	113.6	2.79
$Na(NH_3)_4$	2.477	1.019	112.9	0.0
$Na(NH_3)_4^-$	2.473	1.020	112.8	−0.45

Table 2. CASSCF, CASPT2, and P3+ excitation energies (eV) of $Li(NH_3)_4$ and $Na(NH_3)_4$.

State	E.C.[a]	$Li(NH_3)_4$			$Na(NH_3)_4$		
		CASSCF	CASPT2	P3+	CASSCF	CASPT2	P3+
1^2A_1	$1s^1$	0.00	0.00	0.00	0.00	0.00	0.00
1^2T_2	$1p^1$	0.55	0.72	0.72	0.51	0.65	0.66
2^2T_2	$1d^1$	1.12	1.40	1.40	1.06	1.31	1.32
1^2E	$1d^1$	1.13	1.43	1.43	1.06	1.33	1.34
2^2A_1	$2s^1$	1.28	1.52	1.56	1.22	1.43	1.48
3^2T_2	$2p^1$	1.53	1.79	1.88	1.43	1.67	1.73
1^2T_1		1.61	1.96	1.99	1.52	1.83	1.87
4^2T_2		1.88	2.14	2.26	1.82	2.05	2.18
2^2E		1.94	2.22	2.32	1.87	2.12	2.23
5^2T_2		2.12	2.40	2.56	2.03	2.27	2.50

[a] Electronic configuration.

Table 3. CASPT2 excitation energies (eV) of $[Li(NH_3)_4]_2$ and $[Na(NH_3)_4]_2$.

State	E.C.[a]	$[Li(NH_3)_4]_2$		$[Na(NH_3)_4]_2$
		CASPT2 [b]	CASPT2 [c]	CASPT2 [c]
1^1A_{1g}	$1a_{1g}^2$	0.00	0.00	0.00
1^3E_u	$1a_{1g}^1 1a_{2u}^1$	0.63	0.59	0.42
1^3A_{2u}	$1a_{1g}^1 1e_u^1$	0.77	0.66	0.59
1^1A_{2u}	$1a_{1g}^1 1a_{2u}^1$	1.00	0.92	0.78
1^3A_{1g}	$1a_{1g}^1 2a_{1g}^1$	1.19	1.14	0.96
2^1A_{1g}	$1a_{1g}^1 2a_{1g}^1$	1.18	1.13	0.82
1^1E_g	$1a_{1g}^1 1e_g^1$	1.42	1.30	1.21
1^1E_u	$1a_{1g}^1 1e_u^1$	1.31	1.39	1.03
1^3E_g	$1a_{1g}^1 1e_g^1$	1.53	1.46	1.27
2^3A_{2u}	$1e_g^1 1e_u^1$	1.81	1.76	1.55

[a] Electronic configuration.

[b] CASPT2 optimal geometry used.

[c] DFT/B3LYP optimal geometry used.

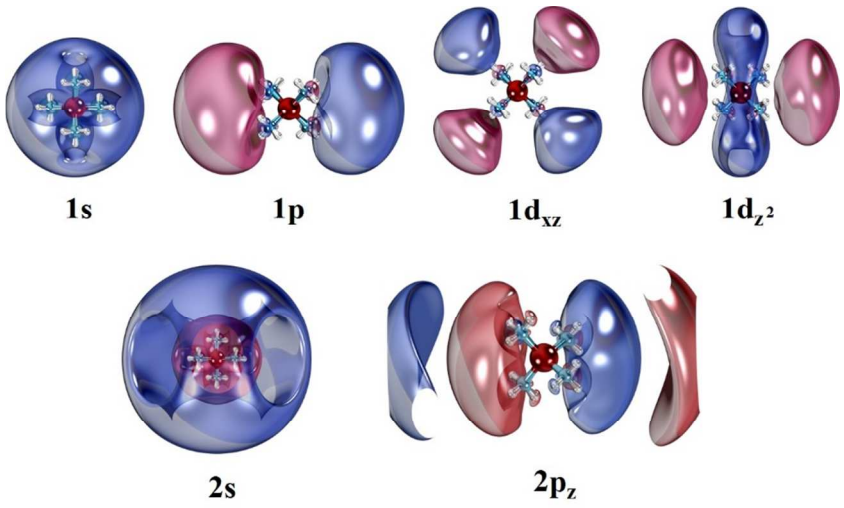

Figure 1. Contours of selected outer orbitals of $Li(NH_3)_4$.

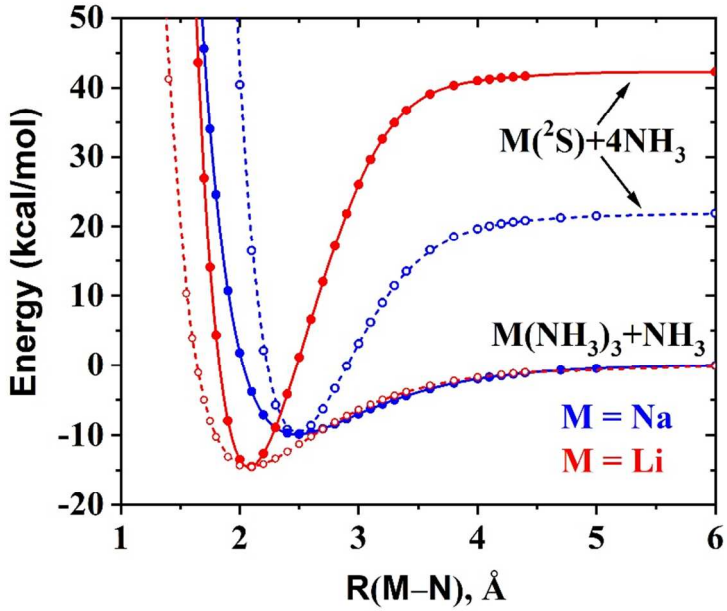

Figure 2. CCSD(T) PECs for the dissociation of one or four ammonia ligands from $M(NH_3)_4$, M = Li, Na.

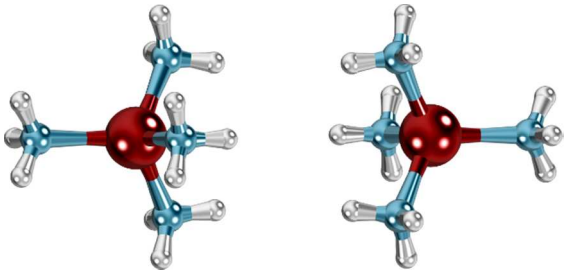

Figure 3. Optimal geometry of $[Li(NH_3)_4]_2$.

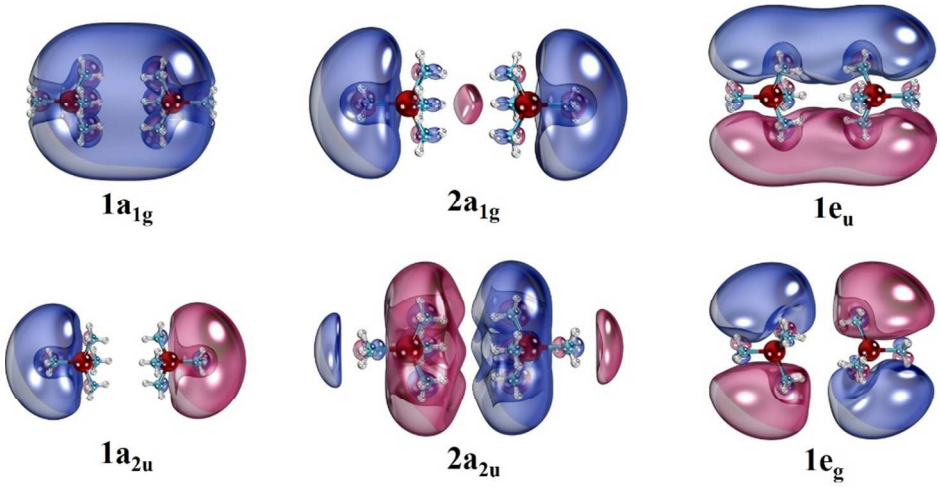

Figure 4. Selected molecular orbitals of $[Li(NH_3)_4]_2$.

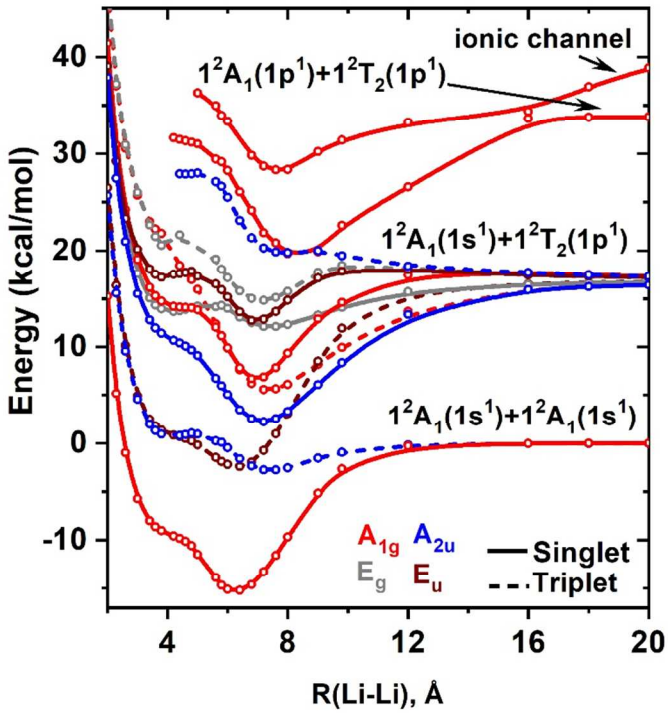

Figure 5. CASPT2 PECs of $[Li(NH_3)_4]_2$ for its dissociation to two $Li(NH_3)_4$ monomers.

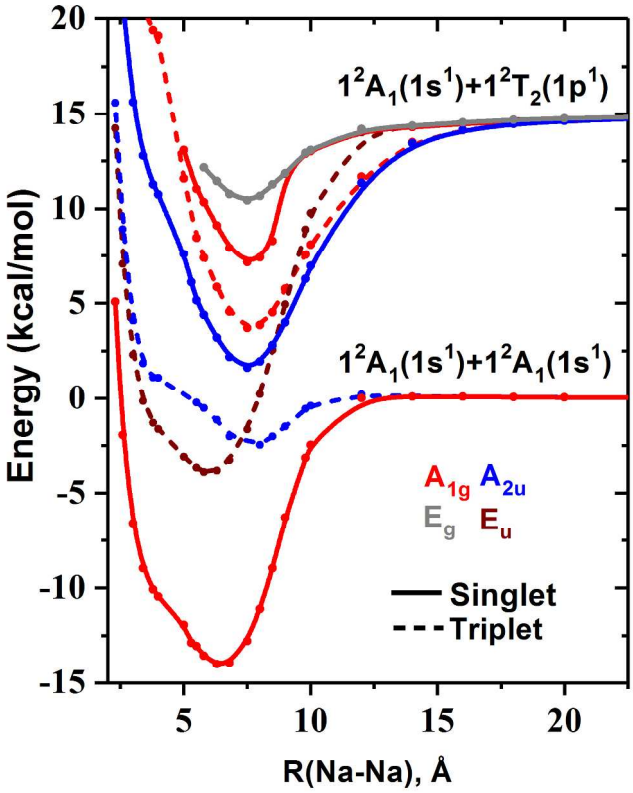

Figure 6. CASPT2 PECs of $[Na(NH_3)_4]_2$ for its dissociation to two $Na(NH_3)_4$ monomers.